

# CASE FILE COPY

INVESTIGATION OF LASER DYNAMICS, MODULATION AND CONTROL

BY MEANS OF INTRA-CAVITY TIME VARYING PERTURBATION

under the direction of

S. E. Harris

Semiannual Status Report

(Report No. 19)

for

NASA Grant NGL-05-020-103

National Aeronautics and Space Administration

Washington, D.C.

for the period

1 February 1973 - 31 July 1973

M. L. Report No. 2192

July 1973

Microwave Laboratory  
W. W. Hansen Laboratories of Physics  
Stanford University  
Stanford, California

17 32A0

1900

1900

1900

1900

1900

1900

1900

1900

1900

# CASE FILE COPY

STAFF

NASA Grant NGL-05-020-103

for the period

1 February 1973 - 31 July 1973

## PRINCIPAL INVESTIGATOR

S. E. Harris

## PROFESSOR

A. E. Siegman

## RESEARCH ASSOCIATES

D. J. Kuizenga

A. H. Kung

J. F. Young

## RESEARCH ASSISTANTS

G. C. Bjorklund

D. W. Phillion

T. Savarino

E. Stappaerts

## I. INTRODUCTION

Work continues on a number of projects aimed at the generation of tunable visible, infrared, and ultraviolet light; and on the control of this light by means of novel mode-locking and modulation techniques. During this period the following projects have been active: (1) the transient mode-locking of the Nd:YAG laser and application of short optical pulses; (2) studies of the sodium-xenon excimer laser; (3) development of techniques for vacuum ultraviolet holography; and (4) studies of multiple photon pumped xenon and argon excimer lasers. Progress on each of these projects is summarized in the following sections.

## II. SUMMARY OF PROGRESS

### A. Transient Mode-Locking of the Nd:YAG Laser and Application of Short Optical Pulses (D. W. Phillion, D. J. Kuizenga, and A. E. Siegman)

In the previous semi-annual report, we presented details of the theory to describe the transient mode-locking in the simultaneously Q-switched and mode-locked cw Nd:YAG laser. We also presented some preliminary experimental results.

During the past six months, we completed several modifications to the laser to improve stability and reliability of the system. We then performed a series of experiments to carefully measure the characteristics of the mode-locked and Q-switched YAG laser. These measurements and the comparison with theory will be submitted to Applied Physics Letters for publication. A pre-print of this paper is attached to this report as Appendix A.

In general, we find good agreement between theory and experiment, and we can now predict the behavior of the mode-locked and Q-switched YAG laser with good accuracy. The main conclusion that we draw is that under reasonable Q-switching conditions, the build-up time is never long enough to approach steady-state mode-locking. However, we also carefully investigated the mode of operation of the laser where the Q-switch in the closed condition does not hold off the laser altogether, but allows it to oscillate at a low level. The modulator is on during this time and mode-locks the laser. When the Q-switch is now opened completely, initial conditions are short pulses which continue with little change through

Handwritten text, likely bleed-through from the reverse side of the page. The text is extremely faint and illegible due to the low contrast and high noise of the scan. It appears to be several lines of a letter or document, but no specific words or structure can be discerned.

build-up and Q-switch pulse. Mode-locked pulses slightly wider than the cw steady-state value are obtained. This mode of operation is stable for Q-switch repetition rates up to 1 kHz . Pulses as short as  $\sim 100$  psec can be generated easily, and increasing the depth of modulation by pulsing the modulator, we expect to generate 50 psec pulses very soon.

At present we are constructing a fast electro-optic switch to select a single mode-locked pulse from each Q-switch pulse. With this we will soon have available a source of single 50 psec pulses, spaced by  $\sim 1$  msec and peak power at  $1.06\mu$  more than 100 kWatts. This can easily be doubled to  $5320 \text{ \AA}$  , and probably doubled again to  $2660 \text{ \AA}$  with good efficiency. Pulse-to-pulse stability will be better than 5%. This will provide us with a very good source for application experiments with these short pulses. We are presently planning some experiments to measure fast lifetime in complex molecules.

This laser system is almost an ideal source for long distance laser ranging and fits very well into the scheme recently described by Golden, et al., "Laser Ranging System with 1 cm Resolution," (Appl. Optics, July 1973).

From the work we have done to date on the mode-locked YAG laser, we realize that it is very difficult to obtain pulses shorter than 50 psec with active mode-locking. We are now starting to look at other ways to mode-lock the cw YAG laser. The cw YAG laser has the inherent advantages of good stability and high repetition rates, and we are trying to find methods to obtain pulse widths that approach the inverse of the line width ( $< 10$  psec) in the cw YAG laser. Using a saturable absorber



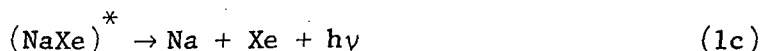
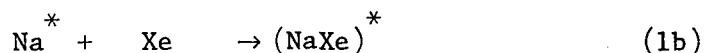


will be the first method to try, but we are looking at other methods to overcome the disadvantages of saturable absorbers. We hope to report some progress here in the near future.

## B. Sodium-Xenon Excimer Laser

(T. Savarino, J. F. Young, and S. E. Harris)

This work is concerned with an experimental investigation into an efficient, tunable source of visible radiation. Previous studies,<sup>1,2</sup> both theoretical and experimental, have shown the feasibility of using molecules composed of alkali earth and rare gas atoms. Molecules, such as lithium xenon and sodium xenon, exist only in an excited state as a result of two body collisions and the following association-dissociation mechanism:



where the wavelength produced by the third reaction lies in the spectral region of 5890 Å to 8000 Å .

This is inherently a very efficient process, because for each molecule formed, one photon of output energy is produced upon dissociation. By way of comparison, some visible laser transitions (such as the argon laser) occur between pairs of excited states separated from each other by a few electron volts. Most of the pumping energy in these processes is taken up in exciting species into a lower excited state, which is typically at a large energy above the ground state. As a result, these

---

<sup>1</sup>W. E. Baylis, "Semiempirical, Pseudopotential Calculation of Alkali-Noble-Gas Interatomic Potentials," J. Chem. Phys. 51, 2665 (September 1969).

<sup>2</sup>A. V. Phelps, "Tunable Gas Lasers Utilizing Ground State Dissociation," Joint Institute for Laboratory Astrophysics Report No. 110, University of Colorado, September 15, 1972.

The first part of the document discusses the importance of maintaining accurate records of all transactions. It emphasizes that proper record-keeping is essential for ensuring the integrity of financial data and for facilitating audits. The text outlines various methods for recording transactions, including the use of journals and ledgers, and stresses the need for consistency and precision in all entries.

Next, the document addresses the issue of reconciling accounts. It explains that regular reconciliation is necessary to identify and correct any discrepancies between the company's records and the bank's statements. This process involves comparing the company's ledger balances with the bank's records and investigating any differences to ensure that both sets of records are in agreement.

The third section focuses on the classification of expenses. It details how expenses should be categorized into different accounts based on their nature and purpose. This classification is crucial for accurate financial reporting and for determining the true cost of various operations. The text provides examples of common expense categories and offers guidance on how to properly allocate costs to these categories.

Finally, the document discusses the importance of reviewing financial statements. It highlights that regular reviews of the balance sheet, income statement, and cash flow statement are essential for understanding the company's financial health and for identifying areas for improvement. The text provides a framework for conducting these reviews and offers tips on how to interpret the data presented in the statements.

processes are inherently inefficient because of the low proportion of output energy to necessary initial excitation energy. Because of the fact that the dissociation mechanism in Eq. (1) occurs between a first excited state and a metastable ground state, this process is inherently far more efficient than any other visible laser mechanism investigated to date.

To date, the experimental work has been done on the sodium-xenon and sodium-helium systems. Experiments aimed at the observation of fluorescence in the band 5890 Å to 8000 Å are being done by optical pumping of the 3s to 3p transition in 1.2 to 1.5 torr of sodium vapor at 750°C in the presence of 160 to 200 psi of xenon. As an experimental control, we have used helium in place of xenon to observe the presence of the pressure broadened sodium D lines around 5890 Å and the occurrence of fluorescence from alkali earth impurities in the sodium used. This is a valid technique because, previously, Baylis<sup>1</sup> had calculated no excited bound states for the possible molecule NaHe. We found that the presence of 160 psi of xenon in the cell decreased the level of fluorescence of the pressure broadened sodium D lines, which leads us to believe that the NaXe molecule may be forming under these conditions.

Presently, we are in the process of building an optical cavity around the system to provide some regenerative gain to the system in the hope that the molecule will exhibit laser action. Upon successful completion, we intend to begin construction of a transversely excited atmospheric system with sodium xenon. We also intend to investigate optical pumping

Handwritten text, likely bleed-through from the reverse side of the page. The text is extremely faint and illegible due to low contrast and significant noise. It appears to be organized into several paragraphs, but the specific content cannot be discerned.

as a means to produce the molecule  $\text{Na}_2$  through the mechanism



The fluorescence expected from this set of molecular transitions is discrete in nature, which is contrasted with the continuum radiation which is expected from the molecule  $\text{NaXe}$ . Future work will also be done on the possible de-activation mechanisms and process cross-sections for both optical and electron beam pumping of the  $\text{NaXe}$  and  $\text{Na}_2$  molecules.

### C. Vacuum Ultraviolet Holography

(G. C. Bjorklund and S. E. Harris)

During this period we have successfully produced holographic gratings using coherent 1182 Å radiation. This represents the first demonstration of holographic techniques in the vacuum ultraviolet region of the electromagnetic spectrum. Polymethyl methacrylate (PMM) was shown to be a suitable photosensitive recording material for VUV holography. Scanning electron microscopy was successfully employed to read-out details in the holograms as small as 1700 Å .

The holographic gratings were produced by recording the linear fringe patterns which result from the interference between a plane object wave and a plane reference wave. The spacing between the linear fringes is given by

$$d = \frac{\lambda}{2n \sin (\theta/2)} ,$$

where  $\theta$  is the angle between the directions of propagation of the plane waves and  $n$  is the index of refraction. Thus, using 1182 Å radiation, a fringe spacing as small as 400 Å may be achieved in LiF, which is transparent to 1182 Å and has  $n \cong 1.7$  .

This type of hologram provides a convenient means for testing the resolution limits of various photosensitive recording materials and the resolution limits of various electron microscopic methods for reading out the hologram. It is important to determine and improve these limits,

since they determine the maximum resolution which may be achieved in holographic microscopy and the maximum fineness of detail which may be achieved in images cast by holographic projection.

In order to achieve resolutions of smaller than an optical wavelength, "grainless" photosensitive recording materials, such as PMM or photoresist, must be employed. During this period we have successfully produced fringes as closely spaced as  $2000 \text{ \AA}$  in Shipley AZ 1350 photoresist with  $2660 \text{ \AA}$  radiation and as closely spaced as  $1700 \text{ \AA}$  in PMM with  $1182 \text{ \AA}$  radiation. Scanning electron microscopy was used to read-out these fringes. Judging from the sharpness of the scanning electron micrographs of these fringes, the resolution limit of this method of holographic read-out is less than  $200 \text{ \AA}$ . Work is now in progress to produce  $400 \text{ \AA}$  fringes in PMM with  $1182 \text{ \AA}$  radiation.

PMM and positive working photoresists such as Shipley AZ 1350 respond to exposure with enhanced solubility. The development procedure consists of placing the exposed medium in a solvent which dissolves away the exposed surface. The local dissolution rate then depends on the previous local exposure intensity. Thus the surface of the medium is etched in a pattern which duplicates the original exposure intensity pattern. When the exposure intensity pattern consists of linear fringes, the fringes are recorded as a period surface relief pattern.

These fringes have direct applications in optics as phase diffraction gratings (both in transmission and, especially useful in the VUV, reflection) and in microelectronics as masks for the fabrication of devices which can be built up from patterns of linear fringes (interdigital



transducers and reflective gratings for acoustic surface waves).

The coherent 2660 Å and 1182 Å sources were obtained as the 4th and 9th harmonics respectively of the 10,640 Å Nd:YAG laser line. Cascaded harmonic generation stages in separate crystals of KDP were used to produce the 2nd, 3rd, and/or 4th harmonics, and a phase matched mixture of xenon and argon was used to produce the 9th harmonic from the 3rd. The Nd:YAG laser/amplifier system produced diffraction-limited 10,640 Å radiation in the form of single pulses of about 30 picoseconds duration, with a repetition rate of up to 10 p.p.s. Each pulse contained about 3 mJ in energy and had a coherence length of about 1 cm. The available energy at 2660 Å was about 0.5 mJ per pulse with a coherence length of about 0.5 cm. The available energy at 1182 Å was about 1 μJ per pulse with a coherence length of about 0.3 cm. (All work with 1182 Å radiation was performed in a helium-purged glove box).

The necessary exposure for development of Shipley AZ 1350 photoresist by 2660 Å radiation was found to be about 5 mJ/cm<sup>2</sup> and the necessary exposure for development of PMM by 1182 Å radiation was found to be about 100 mJ/cm<sup>2</sup>. Thus the largest holograms which could be produced with a single pulse with our available energies was 3 mm × 3 mm with 2660 Å radiation, and 0.03 mm × 0.03 mm with 1182 Å radiation. The use of a single picosecond duration pulse of course dramatically reduces the requirements for stability of the holographic set-up. We found, in addition, that as many as 1000 separate pulses at repetition rates of about 5 p.p.s. could be used to expose much larger holograms without taking special pains to produce an extremely stable holographic set-up. Thus we were able to produce holograms as large as 0.2 mm × 1 mm with 1182 Å radiation.

Work is presently in progress to determine the resolution limit of PMM by means of producing successively finer patterns of linear fringes. PMM has been shown to be sensitive to soft x-ray radiation. It is highly likely that PMM is sensitive to the entire range  $10 \text{ \AA} \leq \lambda \leq 1182 \text{ \AA}$  of the electromagnetic spectrum. Thus if PMM is capable of recording very fine fringes, it will then be a suitable photosensitive recording medium for recording diffraction-limited holographic micrographs with resolution on the order of a vacuum ultraviolet wavelength.

During the next period we also hope to record far-field Fraunhofer holograms of very small objects using  $1182 \text{ \AA}$  radiation. This method does not require a separate reference wave and is applicable to any object which consists of small, concentrated spots on a mostly transparent background. All that is required is to illuminate the object with a coherent wave and place the holographic recording medium in back of the object. If the medium is separated from the object by at least one far-field distance (equal to several microns for typical objects) then the medium will record the interference between the unperturbed portion of the illuminating wave and the far-field pattern scattered by the object. This hologram can then be read-out by an electron microscope, expanded, and an enlarged image reconstructed using a visible wavelength laser to illuminate the expanded hologram. Alternatively, since the far-field pattern is merely the Fourier Transform of the object transmittance pattern, computer methods could be used to reconstruct the object image from the electron micrograph of the hologram. Ultimately, we hope to use this method for producing very high resolution holographic micrographs of biological subjects such as viruses and single cells.

D. Stimulated Emission in Multiple Photon Pumped Xenon and Argon Excimers

(S. E. Harris, A. H. Kung, E. A. Stappaerts, and J. F. Young)

During this period we used multiple photon absorption of laser radiation at 2660 Å and 3547 Å to pump excimers of Xe and Ar. Line narrowing was observed in bands ~ 100 Å wide, centered at 1730 Å and 1260 Å, respectively.

Although it is not possible to conclude that there is net gain, this is very likely because the same gases pumped with an electron beam do show net gain (Ref. 3,4 in Appendix B). If this turns out to be true, high efficiency Xe and Ar excimer lasers could be built using optical rather than electron beam pumping, which in many cases is considerably simpler.

This kind of experiment will also reveal a lot of new information on complicated excimer reactions which are still only incompletely understood.

The results of the experiment are to be published in Applied Physics Letters and are included in Appendix B of this report.

Work on this project was jointly supported by the Atomic Energy Commission, Air Force Cambridge Research Laboratories, and the Office of Naval Research.

APPENDIX A

SIMULTANEOUS MODE-LOCKING AND Q-SWITCHING

IN THE CW Nd:YAG LASER<sup>\*</sup>

by

D. J. Kuizenga, D. W. Phillion, T. Lund,<sup>†</sup> and A. E. Siegman

Microwave Laboratory  
Stanford University  
Stanford, California

ABSTRACT

The theory for transient mode-locking for an active modulator in a laser with a homogeneously broadened line is presented. The theory is applied to Q-switched and mode-locked Nd:YAG lasers and good agreement between theory and experiment is obtained. The main conclusion is that the mode-locking does not approach the steady-state conditions under normal operating conditions. We also present a method to overcome this problem by allowing the laser to pre-lase before the Q-switch is opened. Short pulses approaching the steady-state value are obtained.

---

<sup>\*</sup> This work was jointly supported by the National Aeronautics and Space Administration under NASA Grant NGL-05-020-103 and the Air Force Office of Scientific Research (AFSC), United States Air Force under Contract F 44620-61-C-0053.

<sup>†</sup> Norwegian Defense Research Establishment, Kjeller, Norway.

# SIMULTANEOUS MODE-LOCKING AND Q-SWITCHING

## IN THE CW Nd:YAG LASER

by

D. J. Kuizenga, D. W. Phillion, T. Lund, and A. E. Siegman

Microwave Laboratory  
Stanford University  
Stanford, California

Mode-locking of the cw Nd:YAG laser with active modulators has been studied extensively,<sup>1,2,3</sup> and short optical pulses 40 to 50 psec can be obtained. For many applications, these pulses are more useful at the second harmonic at  $5320 \text{ \AA}$ , but the output from the cw mode-locked Nd:YAG laser is not sufficient to do efficient external SHG. Efficient internal SHG is an additional mechanism to lengthen the pulses, and usually pulses a few hundred picoseconds wide are obtained.

One attractive possibility is to repetitively Q-switch the YAG laser, and simultaneously mode-lock the laser with an active modulator. Q-switching alone will give peak powers  $10^3$  to  $10^4$  times the average power at repetition rates up to 1 kHz, with decrease in peak power at higher repetition rates to  $\sim 20 \text{ kHz}$ .<sup>4</sup> The question now is whether good mode-locking can be obtained under these conditions; i.e., pulsewidths approaching the steady-state value. To investigate this problem one has to understand the transient build-up of the mode-locking from the time the Q-switch is opened to when the actual Q-switch pulse starts. The real question here is whether the mode-locked pulse can make enough

passes through the modulator to approach the steady-state value. To analyze this problem some approximations can be made. In the repetitively Q-switched Nd:YAG laser, the Q-switch build-up time is always much longer than the Q-switch pulse.<sup>4</sup> This means that most of the transient mode-locking occurs during the Q-switch build-up time, and that the mode-locked pulses that have formed during this time continue through the actual Q-switch pulse with very little change in pulsewidth. Consequently, most of the transient mode-locking occurs when there is no saturation of the active medium, the gain is constant, and the axial modes are not coupled together by the homogeneously broadened active medium.

To analyze the transient mode-locking one can initially consider a very simple model of a laser running in a single axial mode and the modulator is turned on at time  $t = 0$ . This model is then applied to the Q-switching situation by making the axial mode slowly time varying (compared to the mode-locking) and by considering multiple axial modes. We will discuss the effects of this later.

The amplitude modulator for the Nd:YAG laser is an acousto-optic modulator,<sup>1</sup> and at  $1.06\mu$  this device operates well into the Bragg diffraction region. The single pass amplitude transmission is then given by

$$f(t) = \cos(\theta_m \sin \omega_m t) \quad , \quad (1)$$

where  $\theta_m$  is the depth of modulation, and  $\omega_m$  is the modulation

frequency. This transmission function also applies to an electro-optic modulator and the recently proposed anti-resonant ring modulator.<sup>5</sup> In all cases, the depth of modulation is proportional to  $\sqrt{P}$ , where  $P$  is the modulator drive power. We will first consider the steady-state conditions. Following the analysis in Ref. 3, the pulsewidth is given by

$$\tau_{p0} = \frac{\sqrt{2 \ln 2}}{\pi} \frac{g^{1/4}}{\theta_m^{1/2}} \left( \frac{1}{f_m \cdot \Delta f} \right)^{1/2}, \quad (2)$$

where  $\Delta f$  is the atomic linewidth and  $g$  is the saturated roundtrip amplitude gain of the active medium. Note that  $\tau_{p0} \propto 1/\theta_m^{1/2}$  and consequently  $\tau_{p0} \propto 1/(P)^{1/4}$ . It was previously shown<sup>3</sup> that  $\tau_{p0} \propto 1/(P)^{1/8}$  for the FM modulator, and it was implied that this was also the case for the AM modulator. This, however, is not the case.

Now consider the transient mode-locking. During the initial build-up of the pulses, we follow the approach of Wang and Davis<sup>6</sup> by considering repetitive passes through the modulator. After  $M$  roundtrips in the cavity, the pulse amplitude is  $E(t) = f(t)^{2M}$ . From Eq. (1), the pulsewidth (FWHM) is given by

$$\tau_p = \frac{1}{\pi f_m} \arcsin \left[ \frac{\arccos \left( 0.5 \frac{1}{4} M \right)}{\theta_m} \right]. \quad (3)$$

After a number of roundtrips, the pulse becomes Gaussian in shape. The pulse shape  $E(t)$  can be expanded in the form

$$E(t) = \left( e^{-a_1 t^2 - a_2 t^4 \dots} \right)^{2M},$$

and for large enough  $M$ , the  $a_2$  term can be neglected, the pulse is Gaussian, and the pulsewidth (FWHM) is given by

$$\tau_p = \sqrt{\frac{\ln 2}{2}} \cdot \frac{1}{\pi} \cdot \frac{1}{\theta_m \sqrt{M} f_m} \quad (4)$$

This equation is valid as long as the pulsewidth is long compared to the steady-state value; i.e., the spectral width is narrow enough that it is not effected by the linewidth, and hence none of the laser medium parameters appear in this equation.

To consider the transition from the long pulses given by Eq. (1) to the steady-state value, the linewidth has to be taken into account. This can be done by extending the previous steady-state analysis.<sup>3</sup> Instead of requiring a self-consistent solution after one roundtrip, we still assume a Gaussian pulse of the form  $e^{-\alpha t^2}$ , but we now allow a change  $\Delta\alpha$  per roundtrip in  $\alpha$ . This leads to a differential equation that can be solved, and after  $M$  roundtrips, the pulsewidth is given by

$$\tau_p = \tau_{p0} / [\tanh KM]^{1/2}, \quad (5)$$

where

$$K = 4 \sqrt{g} \theta_m \left( \frac{f_m}{\Delta f} \right) \quad (6)$$



In Eq. (6),  $g$  is the unsaturated roundtrip amplitude gain at the time the Q-switch is opened; i.e.,  $g = (\bar{N}/2) \ln [1/(1-L)]$ , where  $L$  is the total roundtrip loss in the cavity, and  $\bar{N}$  is the normalized population inversion. From the properties of the tanh function, the pulsewidth is within 5% of the steady-state value when  $KM \geq 1.52$  or for

$$M \geq \frac{0.38}{\sqrt{g} \theta_m} \left( \frac{\Delta f}{f_m} \right) \quad (7)$$

The important parameter we find here is the ratio  $\Delta f/f_m$ , which for the Nd:YAG laser is always on the order of  $10^3$  and it will always take a number of roundtrips of this order or more to approach the steady-state pulsewidth.

The Q-switch build-up time can be estimated from a solution of the single axial mode rate equations.<sup>4</sup> The addition of the mode-locking and multimode operation does not significantly change this build-up time. The equations and details of the calculations will be published later, but the important conclusion that one obtains from this is that the steady-state mode-locking conditions can only be achieved when the laser is very close to threshold. In practice, this can only be approached by running the Q-switching at a sufficiently high repetition rate so that the population inversion does not build up too far above threshold. This gives low peak power and problems with pulse-to-pulse stability.

The experimental set-up to investigate the properties of the mode-locking and Q-switching is shown in Fig. 1. The acousto-optic Q-switch<sup>4</sup> is driven at 25 MHz, with an opening time of  $\sim 400$  nsec. The acousto-optic

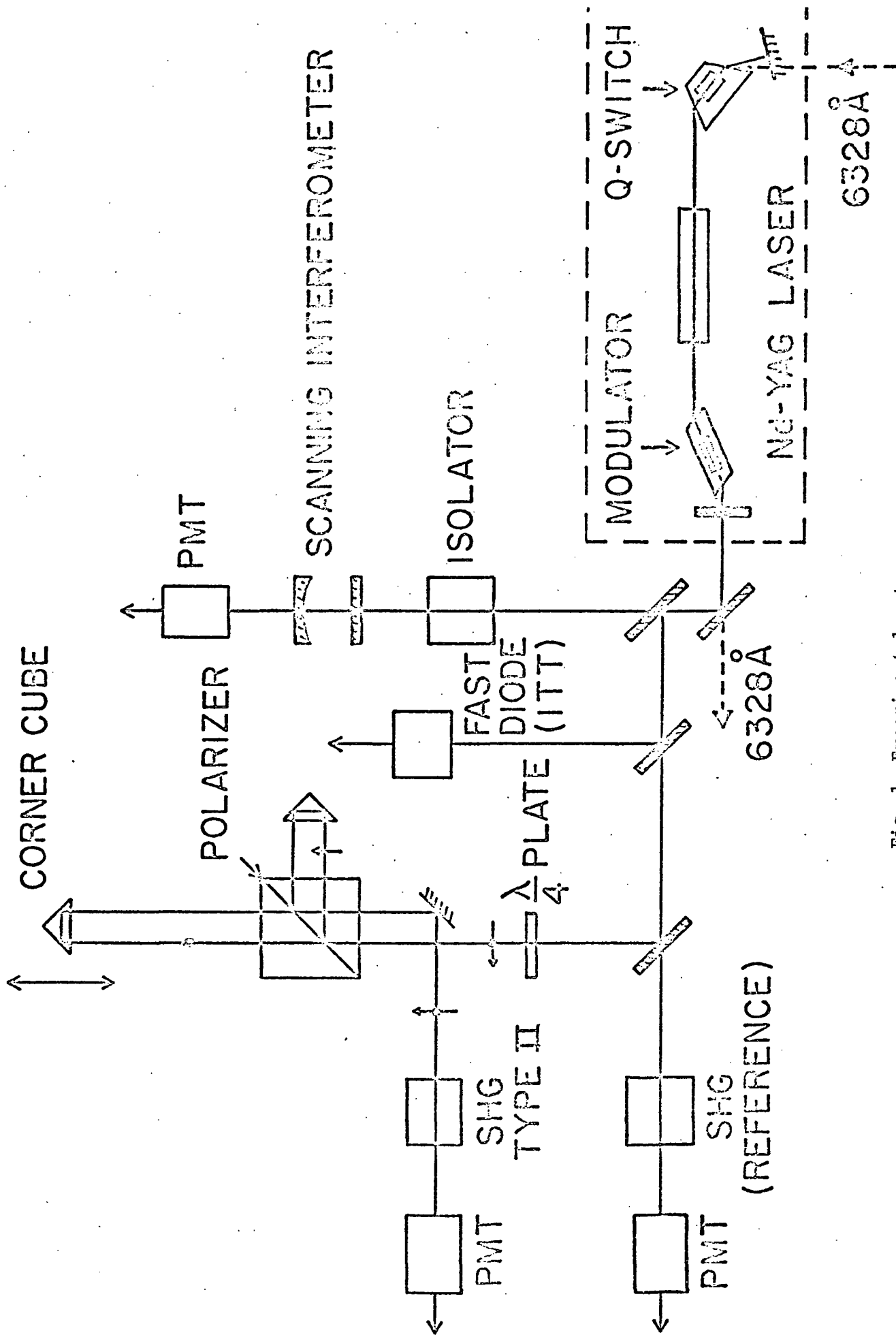


Fig. 1--Experimental set-up.

modulator is driven at 106 MHz, with a maximum depth of modulation as defined by Eq. (1) of  $\theta_m \simeq 0.7$ . A 6328 Å He-Ne beam is passed through the laser coaxially with the 1.06μ beam. This is used to determine exactly when the Q-switch opens to measure build-up times accurately. The 6328 Å is also used to measure the depth of modulation by measuring the average power in the undiffracted and Bragg diffracted beams of the modulator. The YAG laser was operated with a 18.6% output coupler and has an additional 7.4% roundtrip loss. The maximum cw output power was more than 3 watts TEM<sub>00</sub>, linearly polarized. All the experiments were done at the one watt level, which occurred at 50% above threshold. In addition to a scanning interferometer and fast diode, an optical correlator was used to measure the pulsewidths.<sup>7,8,9</sup> Using the polarizer as a beamsplitter and type II SHG, there is no background signal in the correlation function when the pulses do not overlap, and there is also no modulation on the correlation function due to interference terms. Noise from the laser was eliminated by getting a reference SHG signal and taking the ratio of it and the correlator output.

We first studied the cw mode-locking behavior of the AM modulated laser. The correlator plots were very smooth and almost perfectly Gaussian, and provided an accurate pulsewidth measurement. The pulsewidth and the bandwidth are plotted as a function of depth of modulation in Fig. 2. The functional dependence on  $\theta_m$  is as predicted by theory, and Fig. 2 shows that the bandwidth is slightly wider than theory predicts ( $\Delta f = 120$  GHz for theoretical predictions). We get a pulsewidth-bandwidth product of 0.48 while theory predicts 0.44.

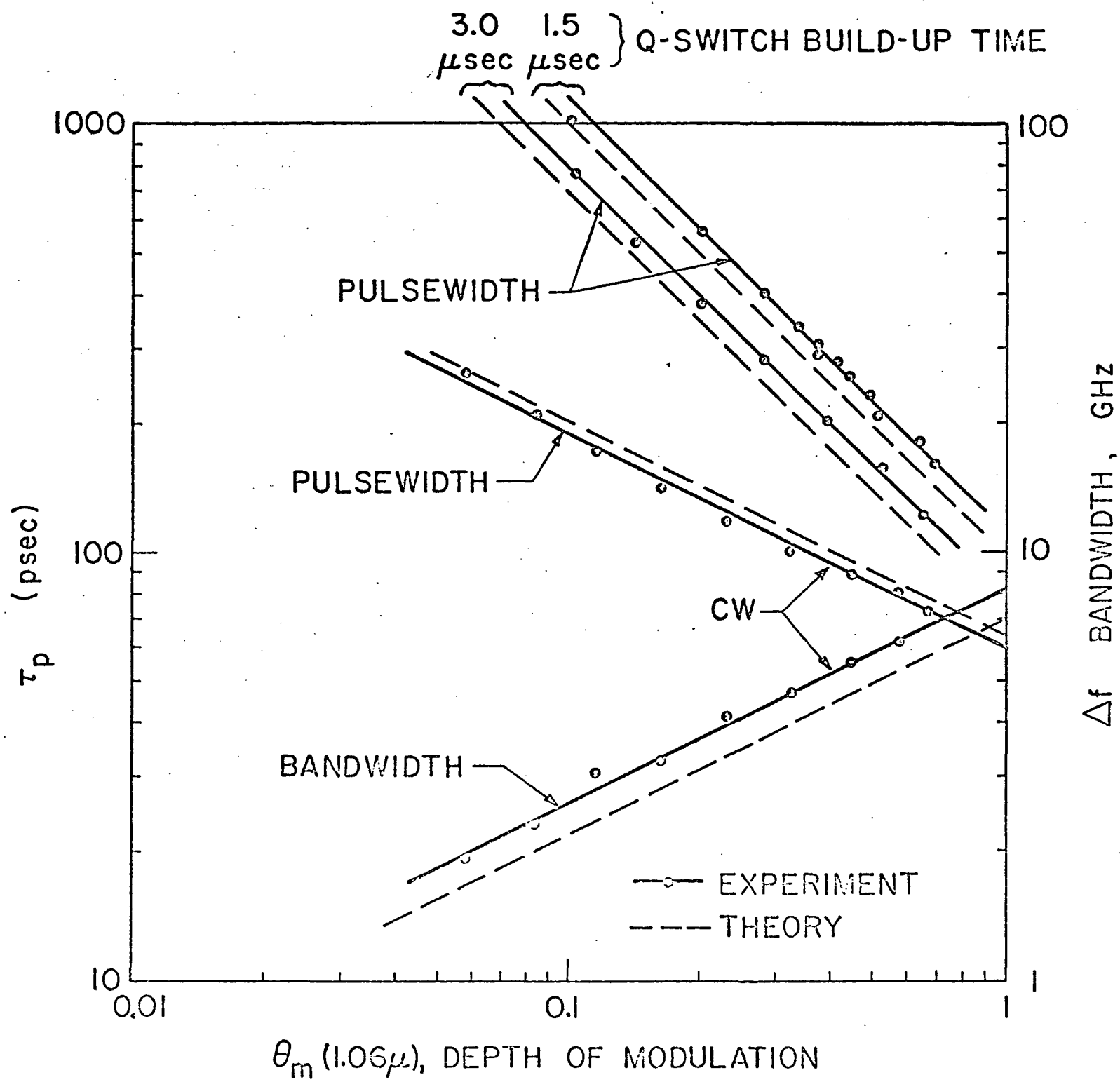


Fig. 2--Pulsewidths and bandwidths as a function of depth of AM modulation for cw and Q-switched YAG laser.

In the transient mode-locking, data was taken by keeping the build-up time ( $\tau_B$ ) constant, and varying the depth of modulation ( $\theta_m$ ) or keeping  $\theta_m$  constant and varying  $\tau_B$ . In all these experiments, the pump power was kept constant, and the build-up time was changed by changing the Q-switch repetition rate.<sup>4</sup> We only used the correlator to measure pulsewidth, and some typical correlator plots are shown in Fig. 3. In the first trace there is no mode-locking. We clearly see the coherence spike with the required 2:1 peak-to-background ratio. This coherence spike appears because of the random phases of the many axial modes. This has been discussed by several authors.<sup>10,11</sup> We have recently completed an analysis to relate the width of the coherence spike to the laser parameters. We find for Q-switching in a laser with a homogeneously broadened line that

$$L_c = \frac{\sqrt{4 \ln 2 Mg}}{\pi} \left( \frac{c}{\Delta f} \right), \quad (8)$$

where all the parameters are the same as defined for the mode-locking. We have verified this expression for pure Q-switching in the Nd:YAG laser, and will publish these results later. The other two traces on Fig. 3 show the correlator traces for various depths of modulation. For weak modulation the background shoulder is wide compared to the coherence spike, and the pulsewidth can be measured easily. For strong modulation, the width of the shoulder becomes comparable to the coherence spike, and we go further out in the wings to obtain a good measure of the pulsewidth as shown in Fig. 3. The results where we keep the build-up



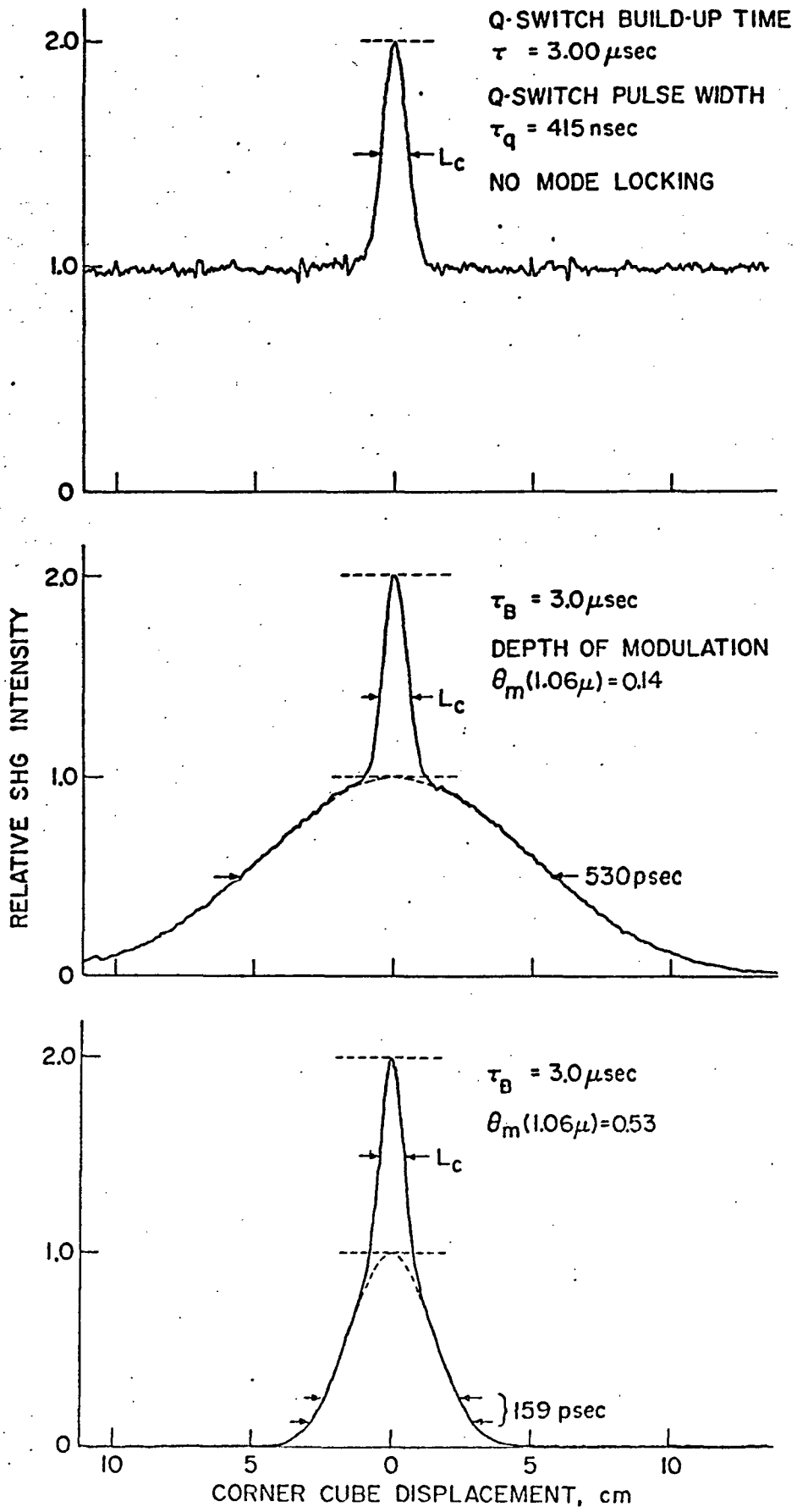


Fig. 3--Typical correlator traces for simultaneous mode-locking and Q-switching.

time constant are shown in Fig. 2, for two build-up times of 1.5  $\mu\text{sec}$  and 3.0  $\mu\text{sec}$ . We see that the mode-locked pulsewidth is proportional to  $1/\theta_m$ , as predicted by theory, but the theory predicts slightly shorter pulses, as shown in Fig. 2. It is also clear that we have not yet reached the steady-state pulsewidths, and that we require  $\theta_m > 1$  to do this. In Fig. 4 we plot the results where  $\theta_m$  is constant. The dependance on build-up time  $\tau_B$  is not precisely  $1/\sqrt{\tau_B}$  as predicted by theory, and the actual pulses are somewhat wider. We have not approached the steady-state pulsewidth for build-up times as long as 10  $\mu\text{sec}$ .

We note that in all cases the experimental pulses are wider than theory. This is most probably due to the fact that the laser is highly multi-mode instead of single axial mode as assumed in the theoretical model. With this wide bandwidth, there will be group velocity dispersion effects that tend to widen the pulses. We are presently extending the theory to include these effects.

There is another very important mode of operation for the mode-locking and Q-switching. This is where the Q-switch does not hold the laser off altogether and allows it to prelase at a low level.<sup>12</sup> With the modulator running continuously, good mode-locked pulses are formed at this time, and when the Q-switch is now opened completely, these pulses continue through the Q-switch pulse with very little change. The pulsewidths should be given by Eq. (2), with  $g$  the unsaturated amplitude gain when the Q-switch is opened. In Fig. 4 we show the pulsewidth with prelasing for a Q-switch repetition rate of 1 kHz.



The first part of the document discusses the importance of maintaining accurate records of all transactions. It emphasizes that every entry should be supported by a valid receipt or invoice. This not only helps in tracking expenses but also ensures compliance with tax regulations. The second part of the document provides a detailed breakdown of the company's income and expenses for the fiscal year. It includes a comparison between the budgeted amounts and the actual results, highlighting areas where the company exceeded or fell short of expectations. The third part of the document discusses the company's financial position at the end of the year, including its assets, liabilities, and equity. It also provides a summary of the company's performance over the period, including key metrics such as revenue, profit, and cash flow. The final part of the document contains a concluding statement from the management, expressing their confidence in the company's future prospects and their commitment to maintaining high standards of financial reporting.

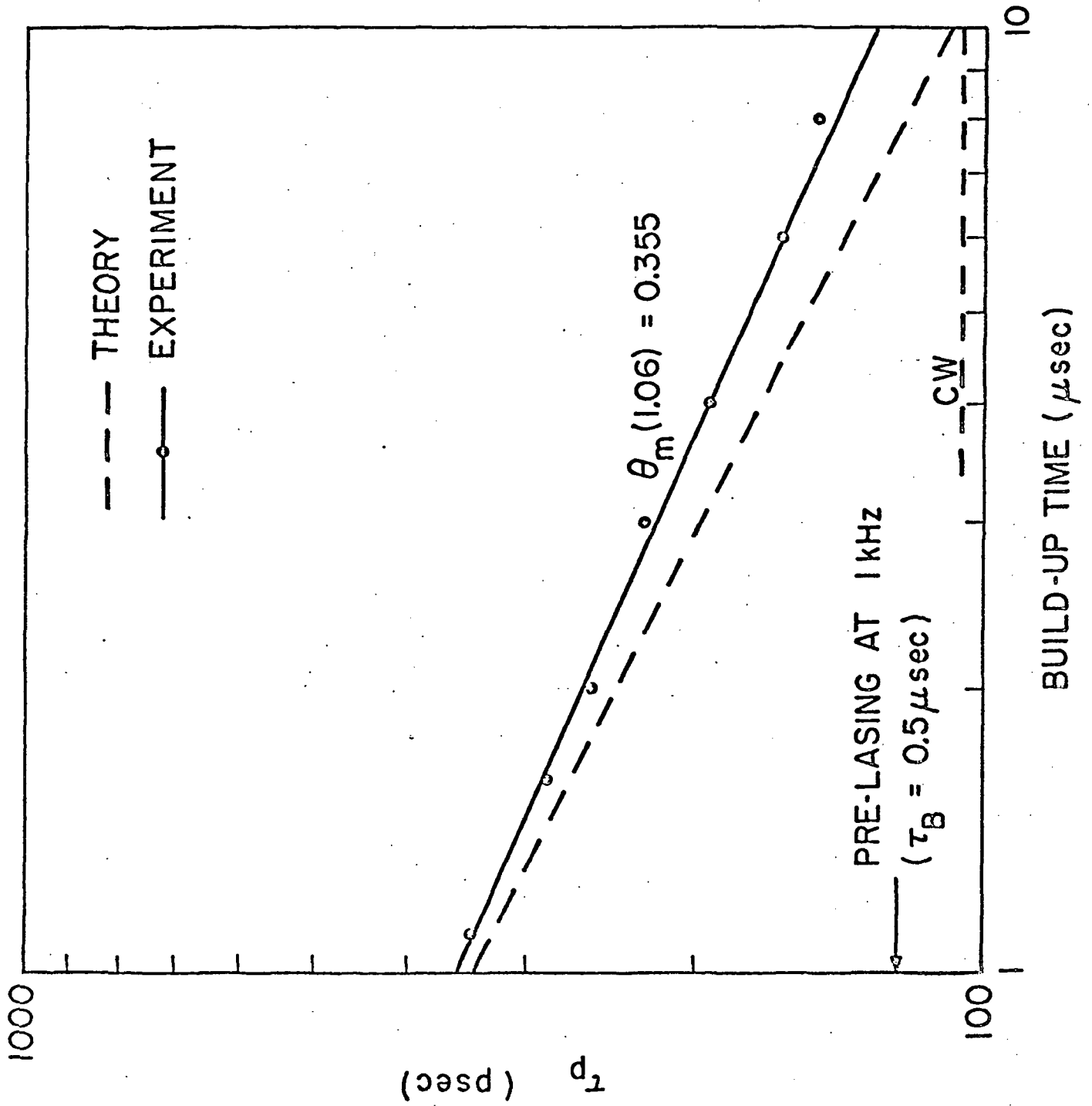
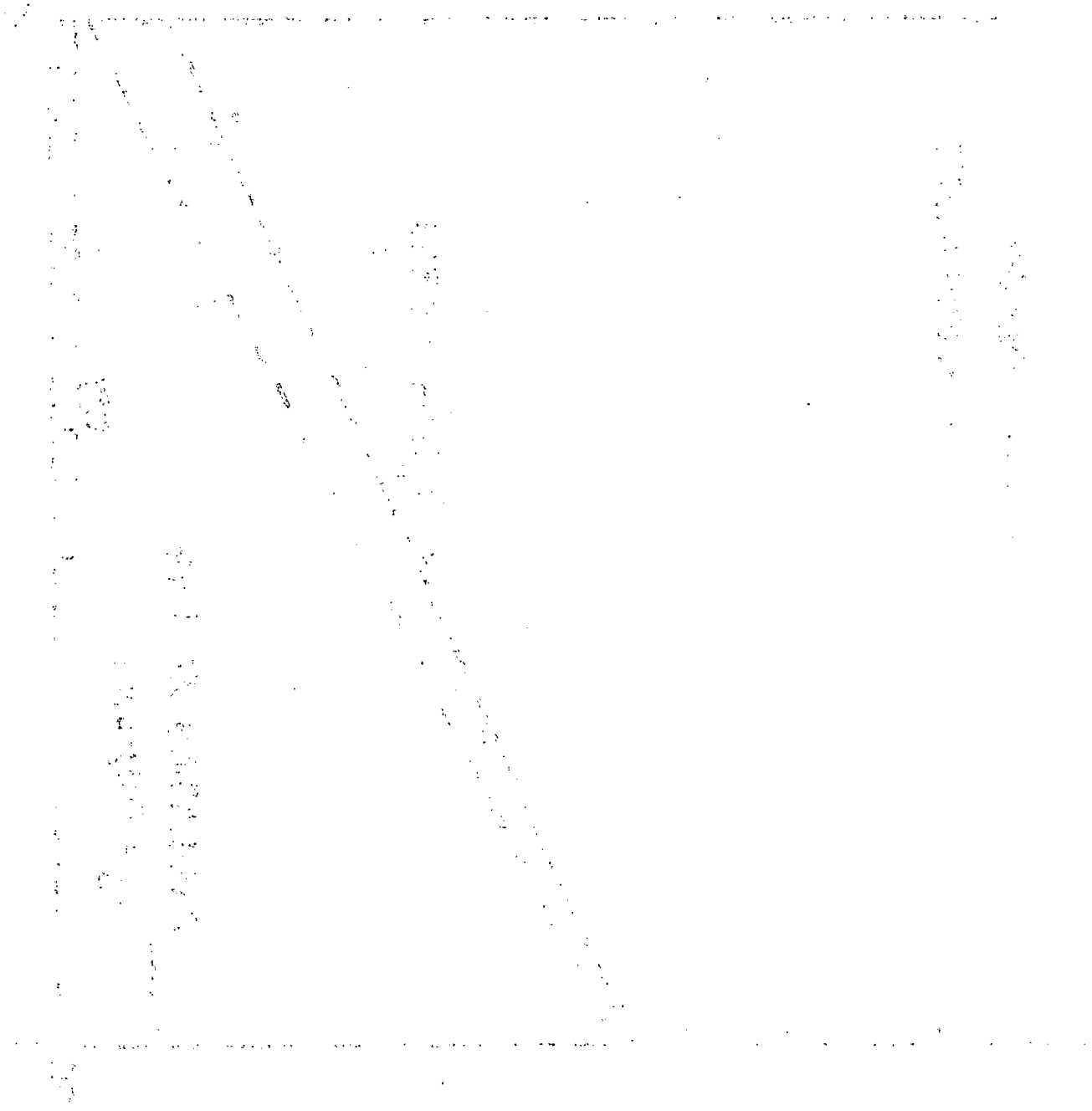


Fig. 4--Pulsewidth as a function of build-up time in the Q-switched YAG laser.



The pulsewidth is wider than the cw value, and this is slightly more than can be explained by using the unsaturated gain in Eq. (2). We also observe that the pulsewidths get shorter at higher repetition rates as expected. However, above 1 kHz the Q-switch build-up time becomes increasingly unstable due to spiking in the prelasing that has not damped out completely.

We can finally conclude that a very simple theory describes the transient mode-locking in the YAG laser quite well. We should also point out that this theory applies to other homogeneously broadened lasers, in particular the mode-locked  $\text{CO}_2$  TEA laser.



## REFERENCES

1. M. DiDomenico, et al., Appl. Phys. Letters 8, 180 (1966).
2. L. M. Osterink and J. D. Foster, J. Appl. Phys. 39, 4163 (1968).
3. D. J. Kuizenga and A. E. Siegman, J. Quant. Elect. QE-6, 694 (1970).
4. R. B. Chesler, M. A. Karr, and J. E. Geusic, Proc. IEEE 12, 1899 (1970).
5. A. E. Siegman, J. Quant. Elect. QE-9, 247 (1973).
6. C. C. Wang and L. I. Davis, Appl. Phys. Letters 19, 167 (1971).
7. D. Gloge and R. Roldan, Appl. Phys. Letters 14, 3 (1969).
8. Archibald W. Smith and Alfred J. Landon, Appl. Phys. Letters 17, 340 (1970).
9. A. Dienes, E. P. Ippen, and C. V. Shank, Appl. Phys. Letters 19, 258 (1971).
10. H. A. Pike and M. Hercher, J. Appl. Phys. 41, 4562 (1970).
11. H. P. Weber and H. G. Danielmeyer, Phys. Rev. A2, 2074 (1970).
12. E. O. Amman and J. M. Yarborough, Appl. Phys. Letters 20, 117 (1972).



APPENDIX B

STIMULATED EMISSION IN MULTIPLE PHOTON PUMPED

XENON AND ARGON EXCIMERS\*

S. E. Harris, A. H. Kung, E. A. Stappaerts, and J. F. Young

(Received May 1973)

In 1966, Basov suggested that stimulated emission in the vacuum ultraviolet (VUV) might be produced by utilizing the continuum emission of rare gas liquids and solids excited by high power electron beams.<sup>1</sup> In 1968, he and co-workers reported VUV stimulated emission in electron beam pumped liquid xenon.<sup>2</sup> More recently, Koehler, et al.<sup>3</sup> and Hoff, et al.<sup>4</sup> reported laser action in high pressure Xe gas pumped by an electron beam.

In this Letter, we report stimulated emission of xenon and argon excimers pumped by multi-photon absorption of laser radiation at 3547 Å and at 2660 Å. Typically, about 25% of the incident pumping radiation is absorbed and effective in producing excimer fluorescence. The fluorescent emission of the xenon and argon excimers centers at 1730 Å and 1260 Å, and has half-power linewidths of about 140 Å and 105 Å, respectively. Line narrowing, and thus stimulated emission, is observed for 2660 Å pumped xenon and argon; though 3547 Å pumped xenon, while yielding comparable excimer fluorescence, does not show stimulated emission.

A schematic of the experimental apparatus is shown in Fig. 1. A mode locked Nd:YAG laser, followed by a single pulse selecting switch and amplifier, produced 1.064 μm pulses with a width of about 25



SECRET

CONFIDENTIAL - SECURITY INFORMATION

CONFIDENTIAL - SECURITY INFORMATION

CONFIDENTIAL - SECURITY INFORMATION

CONFIDENTIAL - SECURITY INFORMATION

CONFIDENTIAL - SECURITY INFORMATION

CONFIDENTIAL - SECURITY INFORMATION

CONFIDENTIAL - SECURITY INFORMATION

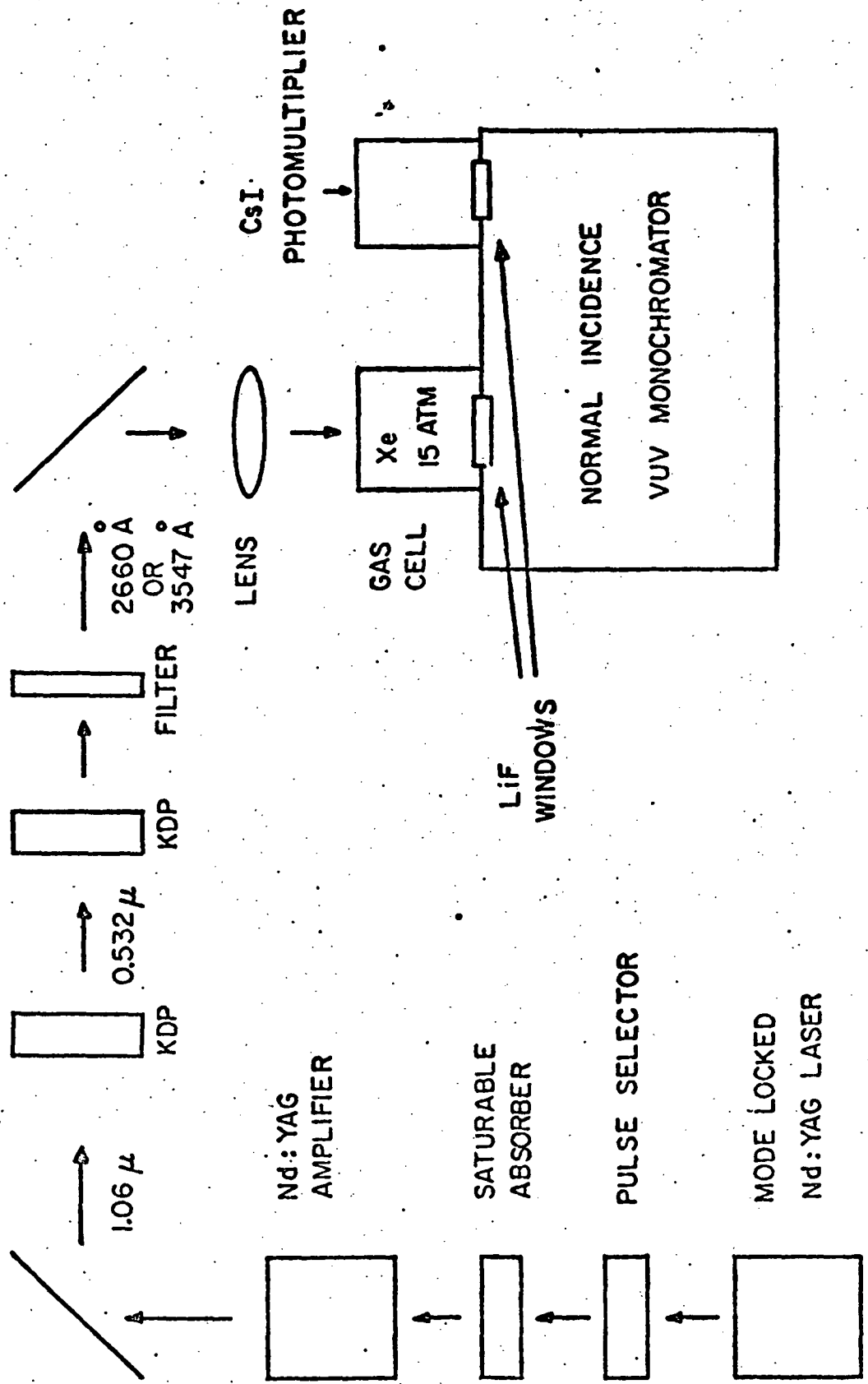
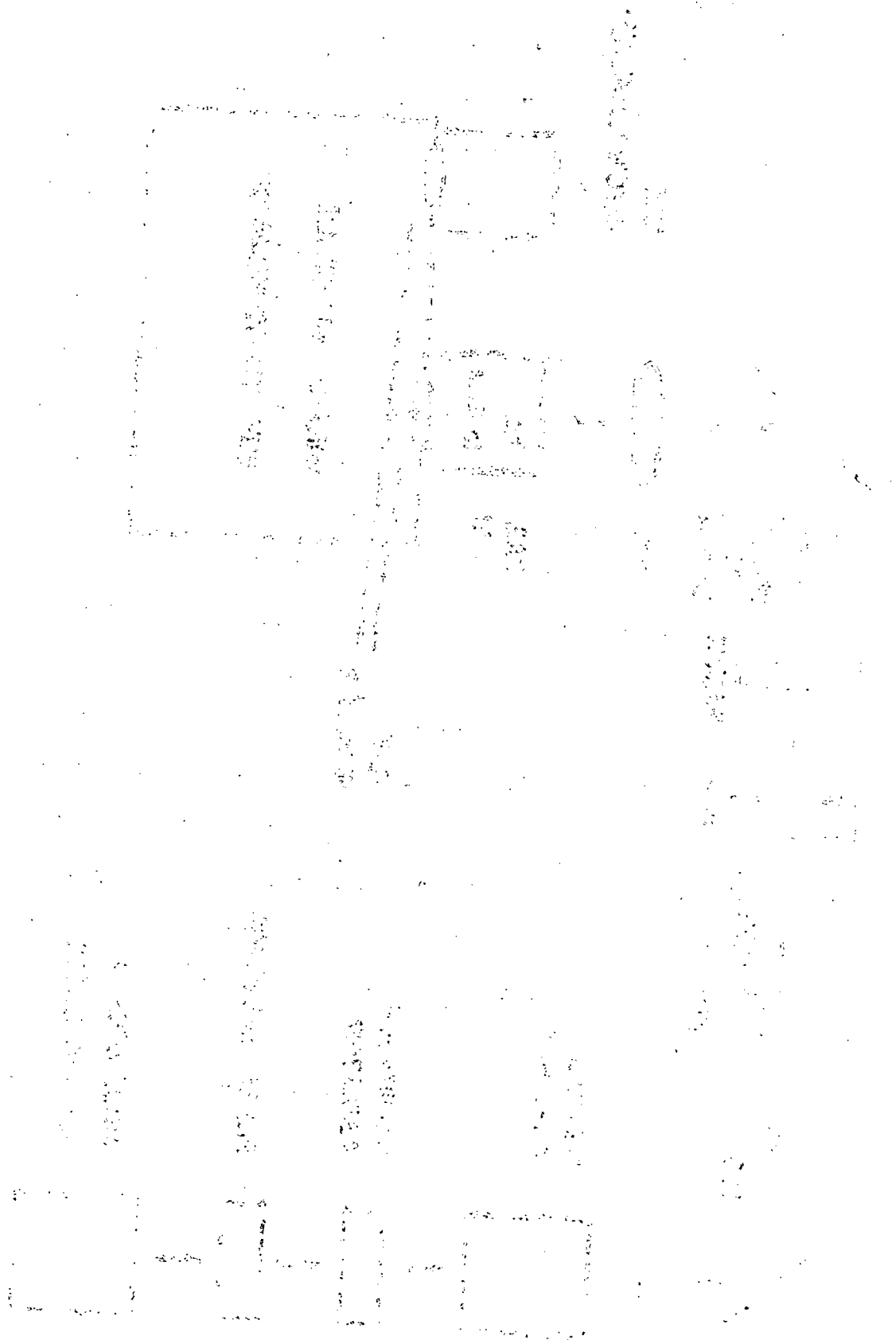


FIG. 1--Schematic of experimental apparatus.



picoseconds and a peak power of about  $1 \times 10^8$  watts. Two KDP crystals were used to convert this radiation to  $3547 \text{ \AA}$  or to  $2660 \text{ \AA}$ . A peak power of about  $1 \times 10^7$  watts was available at either of these frequencies. A gas cell in which the gas pressure could be varied between 0 and 20 atm. was attached to a normal incidence 1 meter McPherson monochromator. The incident laser beam was focussed into the center of this cell to an area of about  $1.4 \times 10^{-6} \text{ cm}^2$ , and thus to a power density of about  $7 \times 10^{12} \text{ W/cm}^2$ . The confocal parameter of the focus and thus the length of the pumped region was about 1.9 mm. The fluorescent emission was detected by an EMR CsI solar blind photomultiplier. Four cases:  $2660 \text{ \AA}$  pumped argon,  $2660 \text{ \AA}$  pumped xenon,  $3547 \text{ \AA}$  pumped xenon, and  $3547 \text{ \AA}$  pumped argon were examined. To establish line narrowing, a comparison of fluorescence collinear with the incident laser beam to fluorescence off-axis with this beam was made.

Figs. 2(a), 2(b), and 2(c) show collinear fluorescence and off-axis fluorescence for the first three of the above cases. Line narrowing (and some structure) is apparent for  $2660 \text{ \AA}$  pumped argon and xenon, while line narrowing does not occur for  $3547 \text{ \AA}$  pumped xenon. Though the percentage line narrowing is not large (20% at the maximum), the results are consistently reproducible to within 4%. Absorption of the incident laser beam was 20%, 50%, and 55% respectively for these three cases. An estimated quantum efficiency from absorbed laser power to total excimer fluorescence of between 30% and 50% was obtained. The signal from  $3547 \text{ \AA}$  pumped argon was weak and it was not possible to make a meaningful comparison of on- and off-axis fluorescence.



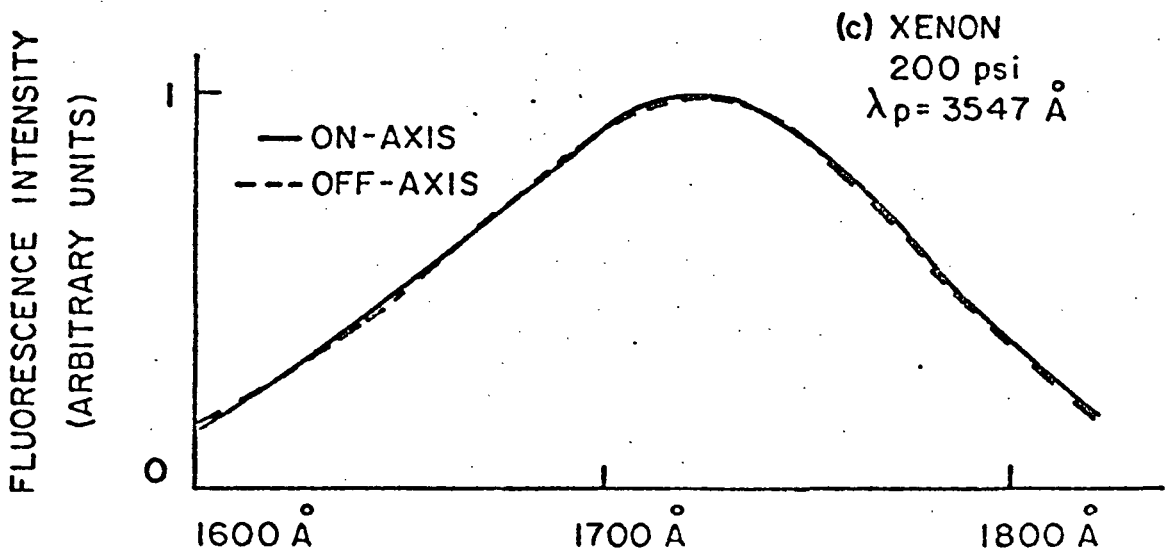
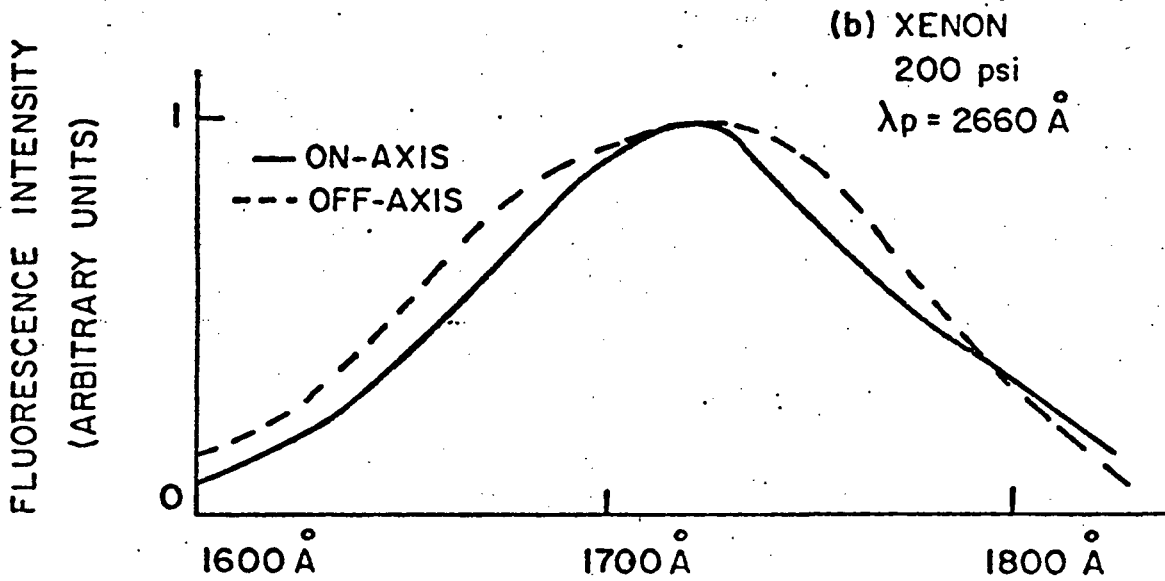
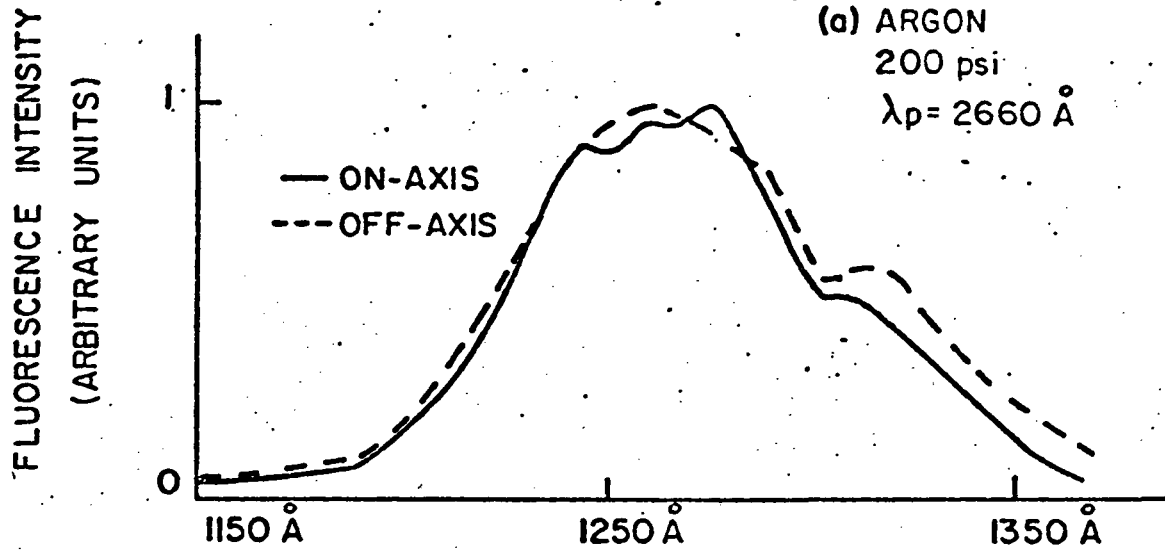


FIG. 2--On-axis and off-axis fluorescence from optically pumped xenon and argon excimers.

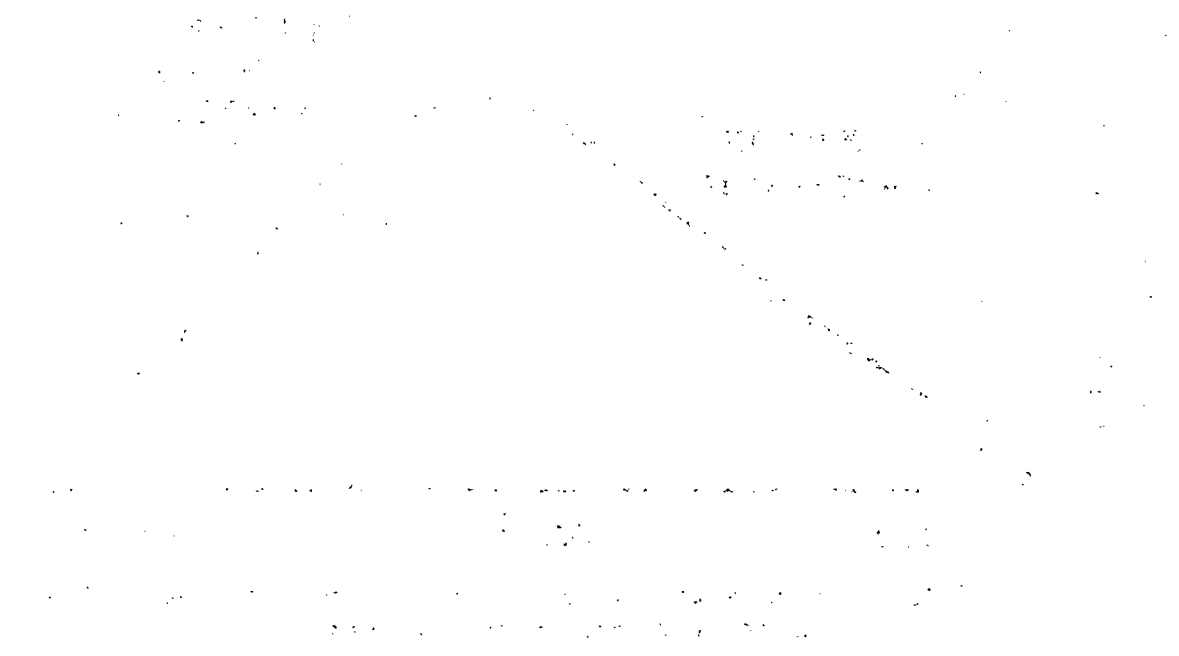
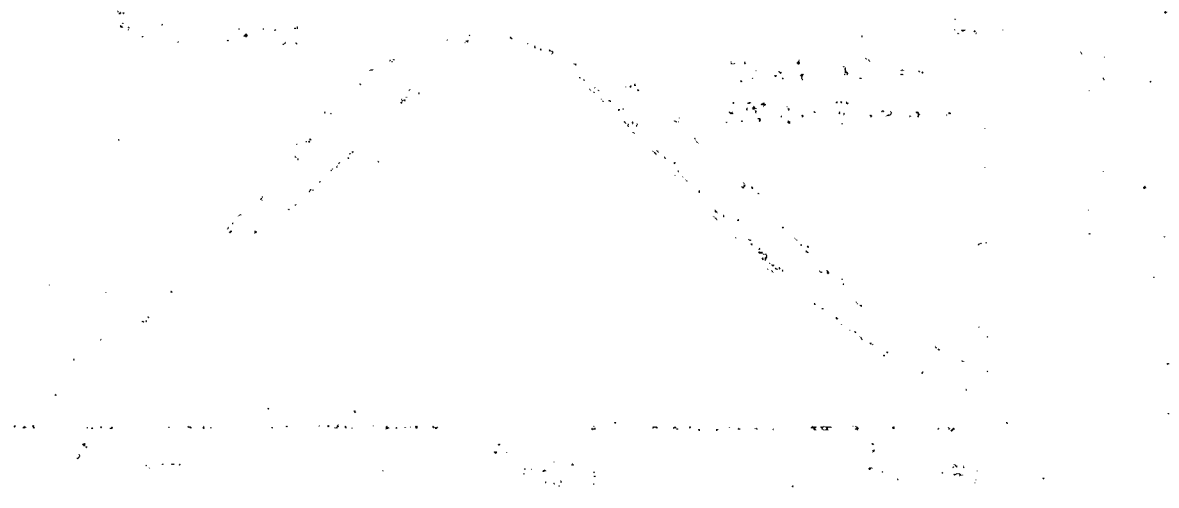


Fig. 3 shows the fractional line narrowing of the collinear fluorescence as a function of the pressure of the inert gas. Normalization is to the linewidth of the off-axis fluorescence, which as expected, is independent of pressure in the range of interest. For both 2660 Å pumped xenon and argon, maximum line narrowing occurs in the vicinity of 2000 p.s.i., probably indicating a reduction in gain due to excimer-excimer deexcitation.<sup>5</sup> It is of interest to note that the maximum line narrowing for 2660 Å pumped xenon occurs at 200 p.s.i., which is very close to the optimum pressure which Hoff, et al.<sup>4</sup> report for electron beam pumped xenon.

The failure to obtain line narrowing for 3547 Å pumped xenon is difficult to explain. The total excimer fluorescence for this case had approximately the same magnitude as in the 2660 Å pumped xenon, and differed only in that it centered about 10 Å toward longer wavelengths. This small shift in center wavelength and the failure to obtain line narrowing indicates that this fluorescence originates from the  $3\Sigma_u^+$  level as opposed to the  $1\Sigma_u^+$  level excited by 2660 Å radiation. The spontaneous lifetime of the  $1\Sigma_u^+$  level is believed to be several nanoseconds, while that for the  $3\Sigma_u^+$  level is several microseconds.<sup>5</sup> The stimulated emission cross section for the  $3\Sigma_u^+$  level is thus much smaller than that for the  $1\Sigma_u^+$  level and is not expected to lead to line narrowing and gain. It is still very surprising to us that multiple photon pumping to levels so high in the energy level structure of the xenon excimer should yield such a selective pumping mechanism.



The first part of the document discusses the importance of maintaining accurate records of all transactions. It emphasizes that every entry should be supported by a valid receipt or invoice. This not only helps in tracking expenses but also ensures compliance with tax regulations. The second part of the document provides a detailed breakdown of the company's financial performance over the last quarter. It includes a comparison of actual results against budgeted figures, highlighting areas of both strength and weakness. The third part of the document outlines the proposed budget for the next quarter, taking into account anticipated changes in market conditions and operational requirements. It also discusses the strategies to be implemented to achieve the budgeted targets. The final part of the document concludes with a summary of the key findings and recommendations. It stresses the need for continued vigilance and proactive management to ensure the company's long-term success and growth.

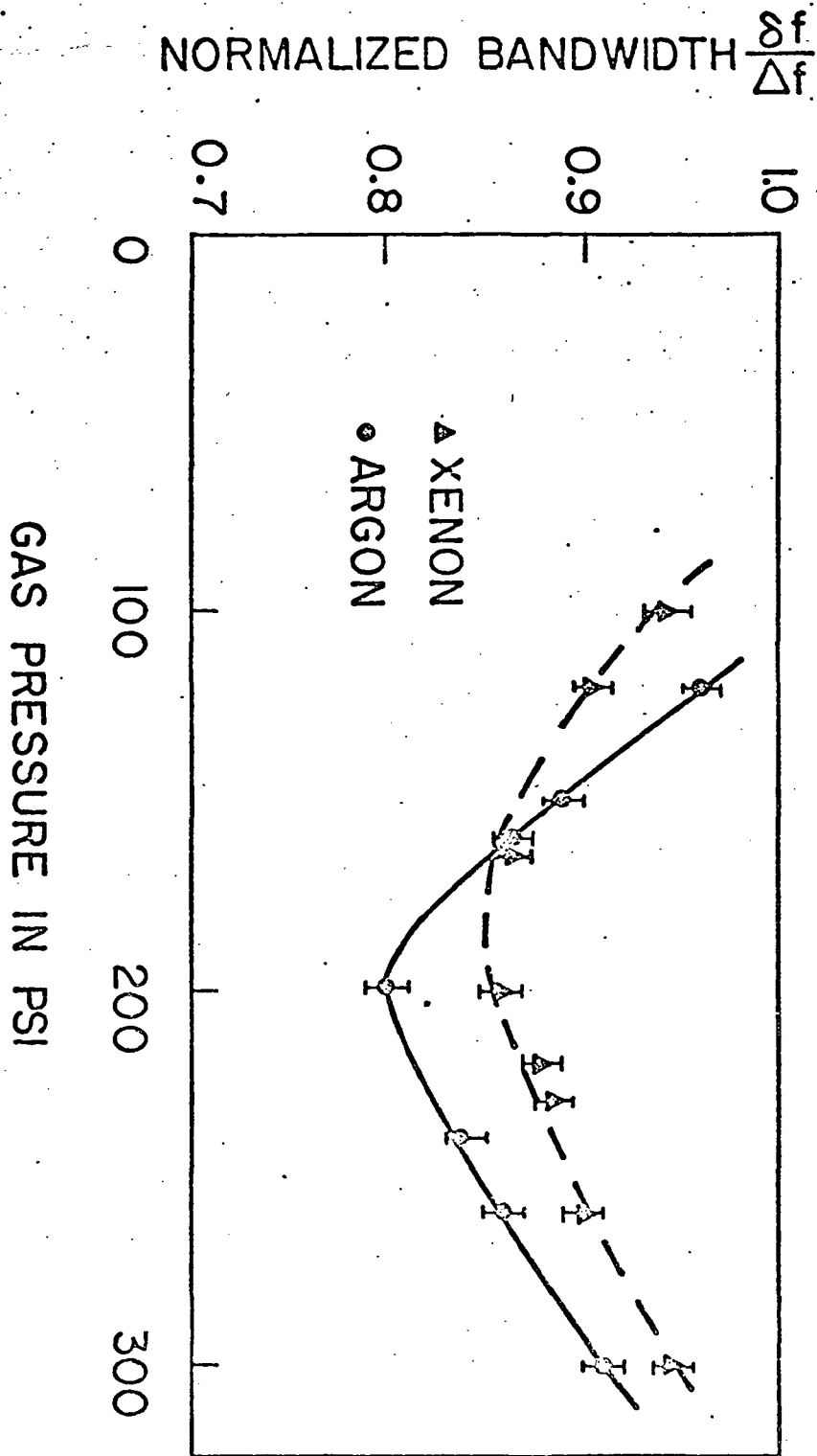


FIG. 3--Normalized emission linewidth vs. gas pressure of on-axis excimer fluorescence.

Beside for the usual multi-photon absorption process where an intense electromagnetic wave causes a single atom to absorb several photons, there is a second and often stronger type of multi-photon process which must be considered. This is a co-operative process where the electromagnetic wave causes the generation of third harmonic radiation which is immediately absorbed. Our calculations, in part based on previous experimental work,<sup>6</sup> show that in 3547 Å pumped xenon that this latter process, i.e., third harmonic generation and absorption, is about 40 times more effective than the more usual direct three-photon absorption process. For 2660 Å pumped xenon, optical absorption varied as input power square, indicating a two-photon absorption process to xenon excimer levels in the vicinity of 1330 Å. Absorption of 3547 Å radiation was proportional to the cube of the input power and thus implies excitation of excimer levels in the vicinity of 1182 Å. Further experiments will be necessary to definitely establish the nature of the absorption process and the extent to which different xenon excimer levels are excited.

Due to distributed loss caused by either ground state xenon atoms, or photo-ionization loss of excited excimers,<sup>7</sup> the directional line narrowing demonstrated in these experiments cannot be used to establish net gain.<sup>8</sup> If we assume the absence of any such distributed loss, then the observed line narrowing of the 2660 Å pumped xenon and argon implies single pass power gains of 2.8 dB and 4 dB, respectively. At the optical power densities employed in these experiments, the excited excimer density exceeds that in the electron-beam pumped experiments of Koehler, et al.<sup>3</sup> and Hoff, et al.<sup>4</sup> With appropriate resonators of other feedback techniques, it is thus likely that multiple photon optical pumping

can substitute for electron-beam pumping in the construction of excimer lasers. When further developed, the technique of multiple photon pumping of excimer systems should also be useful in sorting out excimer formation paths, and for measuring spontaneous decay times and excimer collision rates. It may also allow the construction of practical tunable VUV laser systems.

The authors gratefully acknowledge a number of helpful discussions with J. Aldridge, G. Bjorklund, R. M. Hill, D. C. Lorents, P. W. Hoff, C. K. Rhodes, and A. E. Siegman.

## REFERENCES

1. N. G. Basov, IEEE J. Quant. Elect. 2, 354 (1966).
2. N. G. Basov, O. V. Bogdankevich, V. A. Danilychev, A. G. Devyatkov, G. N. Kashnikov, and N. P. Lantsov, Sov. Phys. JETP Lett. 7, 317 (1968), and N. G. Basov, V. A. Danilychev, and Yu. M. Popov, Sov. J. Quant. Elect. 1, 18 (1971).
3. H. A. Koehler, L. J. Ferderber, D. L. Redhead, and P. J. Ebert, Appl. Phys. Letters 21, 198 (1972).
4. P. W. Hoff, J. C. Swingle, and C. K. Rhodes, "Demonstration of Temporal Coherence, Spatial Coherence, and Threshold Effects in the Molecular Xenon Laser," Opt. Commun. (to be published).
5. C. K. Rhodes, private communication.
6. A. H. Kung, J. F. Young, and S. E. Harris, Appl. Phys. Letters 22, 301 (1973).
7. D. C. Lorents and R. E. Olson, "Excimer Formation and Decay Processes in Rare Gases" (unpublished).
8. A. Yariv and R. C. C. Leite, J. Appl. Phys. 34, 3410 (1963).

## FIGURE CAPTIONS

1. Schematic of experimental apparatus.
2. On-axis and off-axis fluorescence from optically pumped xenon and argon excimers.
3. Normalized emission linewidth vs. gas pressure of on-axis excimer fluorescence.